Proceedings of 8 ICSHMO, Foz do Iguaçu, Brazil, April 24-28, 2006, INPE, p. 795-802.

FLOW AROUND THE ANDEAN ELBOW FROM WRF SIMULATIONS AND P-3 AIRCRAFT MEASUREMENTS DURING THE SALLJEX

John F. Mejia*
Cooperative Institute for Mesoscale Meteorological Studies/Univ. of Oklahoma, Norman, OK

and

Michael Douglas
National Severe Storms Laboratory, NOAA

ABSTRACT

This study focuses on the mesoscale airflow along the eastern slopes of the Bolivian Andes near the city of Santa Cruz. Here the orientation of the Andes changes from NW-SE to N-S (the so-called "Andean bend or elbow"). Here, observations from a NOAA WP-3D research aircraft, obtained during the recent South American Low-Level Jet EXperiment (SALLJEX), showed large horizontal wind gradients on many days and a pronounced mesoscale warm feature in the lower troposphere, associated with cloud-free conditions. The airflow that characterizes these conditions is associated with a northwesterly lower-troposphere wind regime known as the South American Low-Level (SALLJ). A mesoscale cyclonic vortex is also observed on the lee side of the Andean bend, called here the *Andean bend eddy*. This study explores the dynamics of the mean-flow / topography interaction through analysis of the observations and with the aid of numerical simulations of the feature. The simulations are carried out with the WRF model, used with a grid spacing of ~5 km to model the mesoscale structure of the northwesterly flow around the Andean bend. The flow on February 7th 2003 is analyzed with initial conditions from the NCEP Global Tropospheric Analysis (FNL). The flow simulations are compared with the WP-3D observations for general agreement. The likelihood for the development of internal gravity waves, wave breaking and baroclinic vertical vorticity generation is explored for this case study.

1 INTRODUCTION AND MOTIVATION

"The climate of the South American tropical region is characterized strongly by the more or less meridional distribution of the very steep and high Andean mountains" Kleeman (1989)

The occurrence of the South America Low-Level Jet (SALLJ) –typically associated with northwesterly wind conditions, a frequent pattern in the summer circulation- strongly modulates the convection activity over the eastern slopes of the Bolivian Andes and the bordering lowlands (Campetella and Vera, 2002; Berbery et al., 2002). On a continental scale, the effect of this barrier modulates the large-scale circulation over South America. For example, Kleeman (1989) simulated the effect of this orographic barrier on the large-scale circulation using a simple linear two layer model. Kleeman was able to separate the effect produced by this barrier on the dominant baroclinic modes. The main contribution of his work involves the generation of the SALLJ adjacent to the Andes as a result of atmospheric perturbation produced in the Amazonian region (a strong diabatic heating source). These perturbations propagate towards the west and are scattered by the Andes. More detailed studies have explored the interaction of the Andes with the SALLJ. Recently, Campetella and Vera (2002) showed, using different simulation experiments, that the meridional location where the SALLJ occurs is strongly modulated by the intensity of the

* *Correspondent Author: John F. Mejia. 1313 Halley Circle, National Severe Storms Laboratory, Norman, OK, 73069. Tel: 405-579-0873; E-mail: john.mejia@noaa.gov*

cyclonic activity that develops in the lee side of the Andes. In their work, Campetella and Vera (2002) showed, using reanalysis data, that the mechanical effect of the Andes on the airflow is sufficient to reproduce the main observed features of SALLJ.

The effect of the SALLJ on different mesoscale phenomena and its influence on the rainfall and vegetation distribution along the Andean eastern slopes is less well understood. For example, there is a rapid southward decrease in mean rainfall along the lowlands at the foot of the Andean slopes, where the Andes change their orientation near Santa Cruz, Bolivia. At the same elevation, and on relatively flat terrain, the mean precipitation decreases from more than 4000 mm to less than 750mm in a distance of approximately 200 km. Explanations for such major climatological gradients such as this are not found in the meteorological literature. The interaction of the frequent northwesterly wind conditions and the orography, particularly near the sharp change in the orientation of the Andes (the "bend") from NW-SE to N-S (near the city of Santa Cruz), does not seem to have been studied.

Motivation for this study comes in part from our interest in helping ecologists (with whom we have been working) explain the observed climatic gradient of the Andean bend, which is important for explaining the distributions of many species or organisms. The effect of SALLJ events on the cloud field during the austral summer can be observed from simple inspection of the satellite imagery composites shown in Figure 1. A cloud-free zone is commonly observed under the frequent northwesterly wind conditions downstream of the Andean bend (wake zone). Understanding the cloud patterns should in turn help to explain the observed rainfall distribution, and thus the corresponding vegetation patterns.

Additional motivation for our study also comes from direct aircraft measurements made during the South American Low-Level Jet EXperiment (SALLJEX), which provided some of the best observations to date of these meteorological gradients. Observations from a NOAA WP-3D research aircraft obtained during the SALLJEX showed large horizontal wind gradients on many days and a pronounced mesoscale warm feature in the lower troposphere, associated with cloud-free conditions. This study will attempt to explain these observations through the use of a state-of-the-science high-resolution numerical model, the Weather and Research Forecasting (WRF) model. This model is used to simulate the flow around the Andean bend. We then diagnose certain characteristics of the flow.

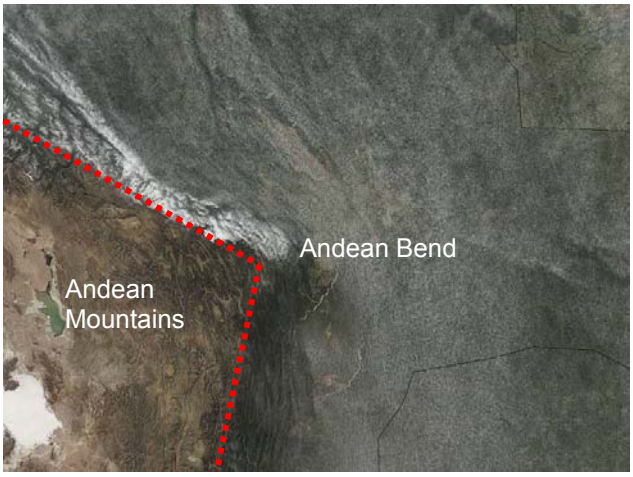

Figure 1 MODIS imagery average for days with northwesterly airflow around the Andean bend during the Austral summer of 2004-5. Relatively cloud-free conditions prevail downstream while high cloudiness is present just upstream (northwest), over the Andean foothills. The white artifact in the lower-left corner is the Uyuni Salt flat (Bolivia). Solid red lines illustrate the large-scale orientation of the Andes.

2 DATA AND METHODOLOGY

Special aircraft measurements were made during SALLJEX along the eastern slopes of the Andean bend and the bordering lowlands. A total of 13 flights, with an average time of 7.5 hours per flight, were made using a NOAA WP-3D research aircraft to measure the three-dimensional structure of the low-level troposphere (from 500 feet AGL to about 700 hPa) and other mesoscale phenomena. Standard variables like wind (all components), humidity, and temperature were collected at one-second resolution during the flights. An example of the flight strategy carried out during the experiment is shown in Figure 2. This figure shows a typical day with strong northwesterly winds (SALLJ event February 7th, 2003), the case chosen for this study. Figure 2a shows a strong horizontal gradient with some return (southerly) flow (hereafter called the *Andean bend eddy*) on the western side of leg C-D. A deeper boundary layer (Figure 2c) is located on the cyclonic shear side of the jet core (Figure 2b). From this figure it

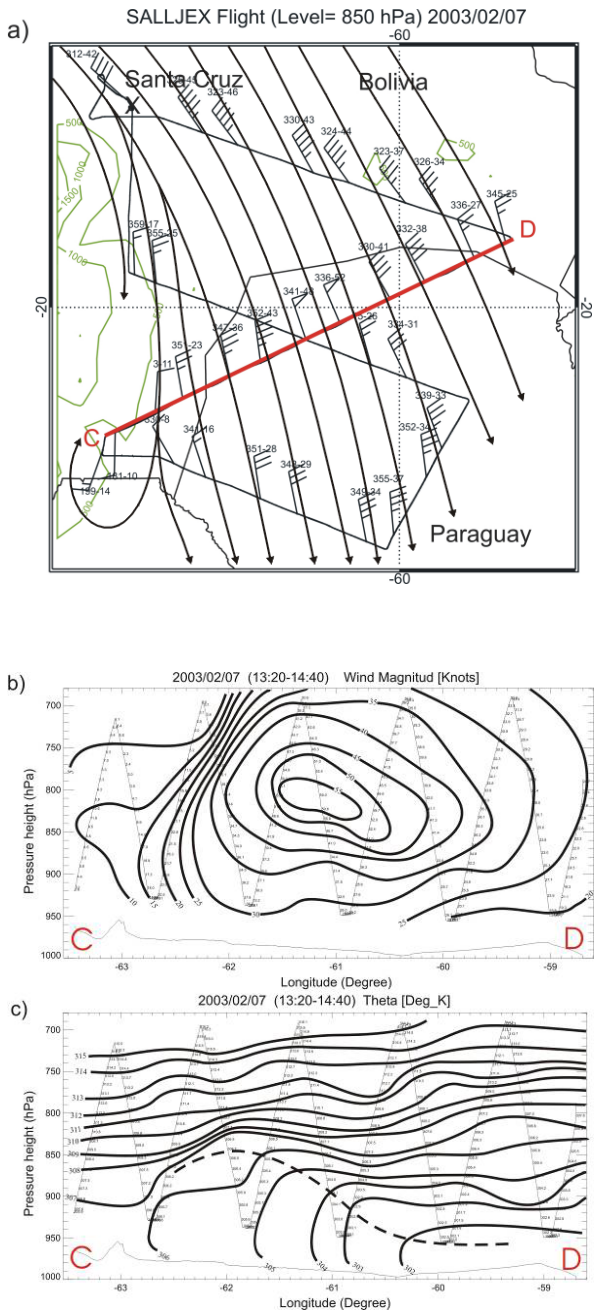

Figure 2 Streamline analysis at 850 hPa of the NOAA P-3 winds (a) and vertical cross sections (b and c) for the February 7th SALLJ event. Panels (b) and (c) shows the porpoising pattern and manual analysis of the wind speed and potential temperature, respectively, along the leg C-D shown in panel (a). Flight started and ended in Santa Cruz, Bolivia. The flight took about 7 hour to be completed.

is obvious that the depth of the mixed-layer varies across the jet near the mountains slope. Details of the observations obtained with the WP-3D aircraft can be found at http://www.nssl.noaa.gov/projects/pacs/salljex/p3/.

Given the lack of routine and densely-spaced upper level observations around the Andean bend, a modeling approach was chosen in order to explore the mesoscale phenomena induced by this topographic feature. Numerical simulations using the Weather and Research Forecasting (WRF) model were run for several of the days on which flights were carried out. These simulations are used to study the processes that are likely to be responsible for the observed cloud field and the effect of orography under the strong winds imposed by the SALLJ. The NCEP Global Tropospheric Final Analysis (1 x 1 degree resolution) (FNL analysis) was used as initial and boundary conditions for the 24 hour runs. The runs started at 00 UTC, approximately 12 hours before the aircraft took off (usually near 12 UTC). This procedure avoids the spin-up problems produced by the mesoscale model. The simulations used an outer coarse grid of 15 km and an inner one-way nested grid of 5km (Figure 3). The domain of the coarse grid includes the upstream flow conditions of the SALLJ, while the nested domain ingests higher-resolution terrestrial fields for the simulations. No sensitivity analysis was performed for the various physical parameterizations contained in the WRF model. The physics schemes activated in all of the runs were: microphysics (Lin et al (1983), longwave radiation (RRTM), shortwave radiation (Dudhia scheme), surface-layer (Monin-Obukhov scheme), land-surface (Noah land-surface model), boundary-layer option (YSU) and cumulus parameterization (Kain-Fritsch).

To illustrate the performance of models such as the WRF, the simulations are compared with independent observations not ingested into either the initial or boundary conditions. The emphasis here is on understanding the effect of the Andean bend on the downstream flow and to evaluate whether the model captures the observed mesoscale patterns in a realistic manner.

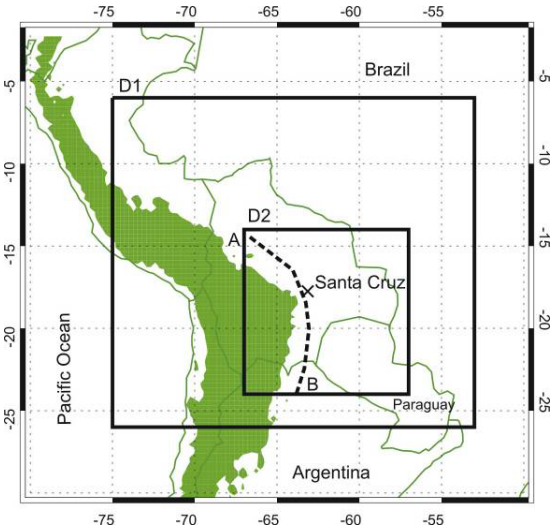

Figure 3 Simulation domains: Coarse grid (D1 - 15 km) and a one way nested grid (D2 - 5 km). The dashed line A-B indicates the location of a cross section used in the analysis along the LLJ. The shaded area represents elevations above 1500 m ASL. Santa Cruz is located on flat land just to the east of the foothills of the Andean Bend.

3 RESULTS

3.1 *SIMULATION RESULTS*

In general, reasonable agreement is seen between WRF simulations and WP-3D observations, especially in the vertical and horizontal structure of the LLJ. The aircraft data was objectively analyzed using a method based on the Barnes successive correction technique (Barnes, 1994). The structures of the LLJ and PBL are illustrated via vertical cross-sections of meridional wind and potential temperature (Figure). The location and magnitude of the LLJ wind maximum in the model resemble the observed values. While the aircraft data show a maximum of 25 ms^{-1}, the model produces a maximum of 20.5 ms^{-1}, 80 km closer to the Andes. Southerly winds are observed by the aircraft and also reproduced in the WRF simulation near the western boundary of the cross section; this feature is part of the Andean bend eddy. As for the potential temperature field, the model run agrees better at levels above the PBL, although it captures major observed features, such as the temperature gradient becoming more enhanced on approaching the Andes. Some lack of vertical and horizontal correlation between the two sections may result from the time lag between the flight segment and the time for the simulation. Although not shown here, five other flight days were simulated with the WRF with generally satisfactory results.

A larger-scale view of the mean-flow / topography interaction when strong low-level northwesterly winds occur in the vicinity of the Andean bend is shown in Figure 5. Figure 5a shows the potential temperature field at 850hPa average over the entire simulation period (24 hr). This figure shows the warmer region of potential temperature close to the eastern slopes of the Andes and downstream of the Andean bend.

3.2 *EFFECT OF THE ANDEAN BEND ON THE AIRFLOW*

Although significant progress in understanding the dynamical processes around complex terrain has occurred in previous decades, the airflow in the vicinity of mountain obstacles is still not well understood, (Blumen, 1990; Smith, 2003). Under some circumstances the airflow around the mountain obstacles can create internal gravity waves, mountain wave breaking, generation of mesoscale vortices, potential vorticity generation, and other local phenomena. The idea that for a given upstream state several downstream states may be possible complicates this kind of study (Goergelin and Richard, 1996). Figure 6 shows a conceptual model of the airflow around the Andean bend. Due to the presence of the Andes, the low-level winds are deflected along the eastern slopes with a significant increase in the wind speed that can be accounted by a variety of synoptic and boundary layer mechanisms (Mejia, preprint http://www.nssl.noaa.gov/projects/pacs/salljex/archive/research/ mejia/ABL.Mejia.htm). Low-level winds cannot rise over the elevated corner and are forced to flow around it. Only under certain circumstances can the air ascend over the bend. For example, if the static stability of the lower atmosphere (gravitational potential energy) is low and the incident wind speed (kinetic energy) is high, then the flow can go over the topography of the bend. Consequently, the condition of whether a given air parcel will go up and over the bend or around is given by the Froude number (*Fr*). *Fr* can be estimated by $U(g\,H\,\Delta\theta\,/\,\theta)^{-1/2}$, where U is the approaching wind speed, θ is the average potential temperature in the layer, and $\Delta\theta$ is the potential temperature increase in the stable layer between the surface and the height of the obstacle H (O'Connor et al. 1994).

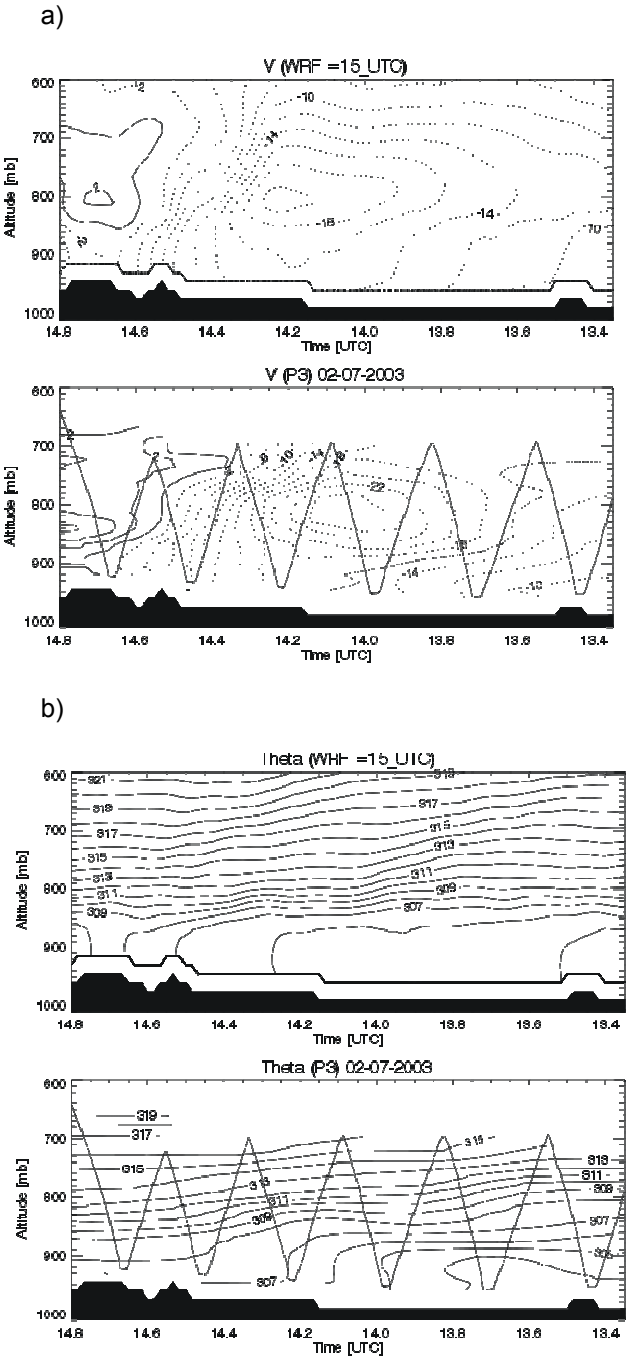

Figure 4 Comparison between WRF simulations and aircraft observations. Cross sections are taken along line C-D shown in Figure 2. (a) Meridional wind component (m s^{-1}) and (b) potential temperature (K). A successive corrections objective analysis scheme based on Barnes technique (Barnes, 1994) was applied to the aircraft data.

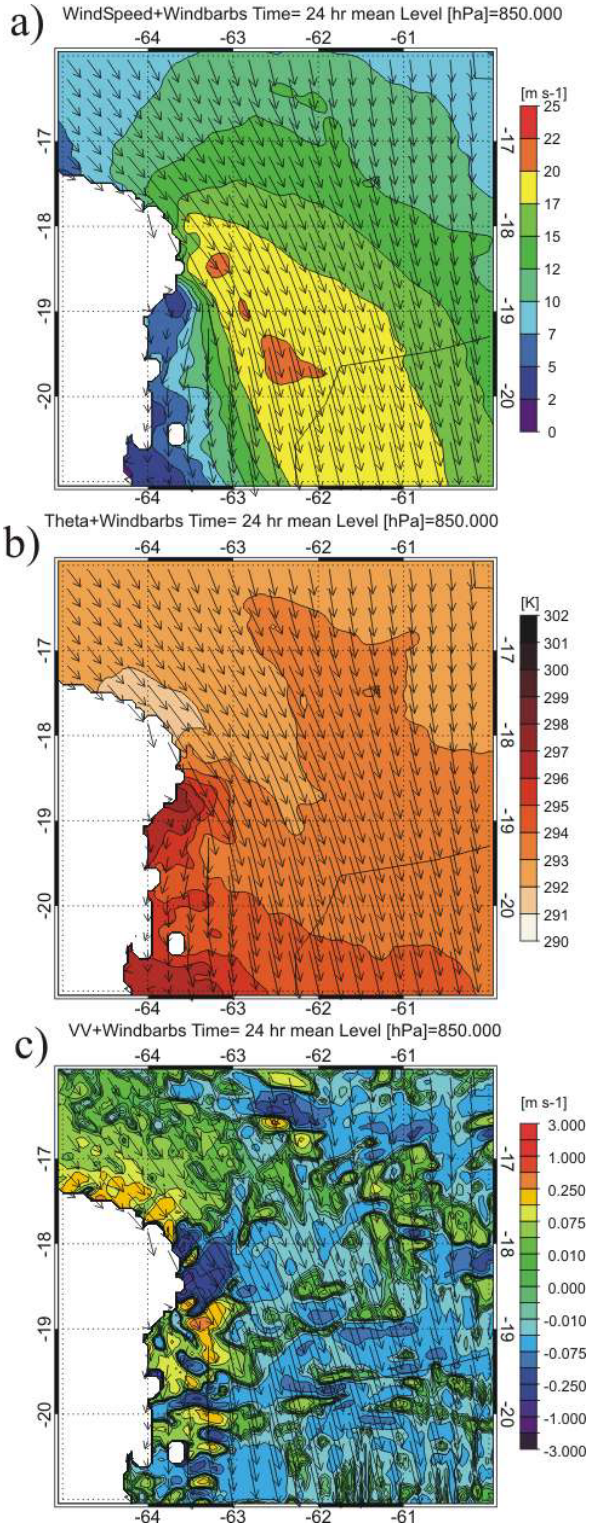

Figure 5 Model simulated (a) wind speed (ms^{-1}) (b) potential temperature (K), and (c) vertical velocity (ms^{-1}) at the 850hPa level for the 24hr run mean values. Superimpose in every map are the horizontal wind vectors at every 5 grid points in either direction.

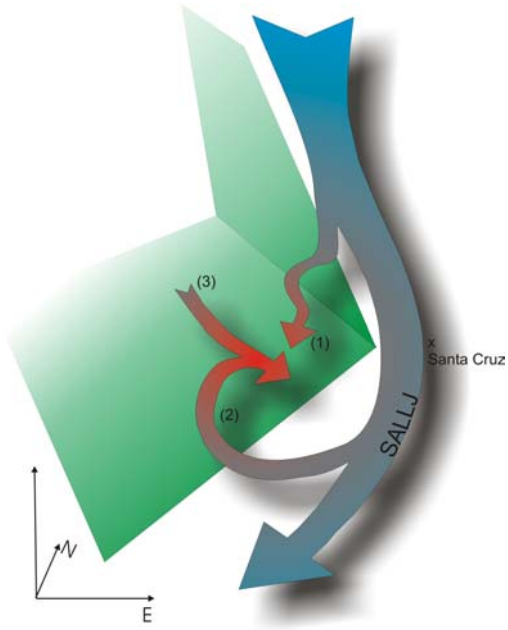

Figure 6 Conceptual model of the flow downstream of the Andean bend under SALLJ events. (1) illustrates the flow over the tilted corner (Andean bend) and posterior wave breaking; (2) the flow of the lee wake region or reversed flow (Andean bend eddy); and (3) downslope flow.

Figure 7 shows a cross section of different simulated variables following a streamline that lies near the surface of the terrain. The Froude number can be roughly estimated for the conditions upstream of the bend (the bend is located right at the point of the highest mountain feature shown in Figure 7, around 4.5 arc_deg from point A) assuming a stable stratified layer, which is not completely true in this case. By doing so, for values of θ=302 K, $\Delta\theta$=2K, H=1140m and U=8 ms^{-1} then Fr=0.9 (indicative of a subcritical flow). The condition of a stable layer is basically violated since θ is nearly constant in the layer upstream and behind the obstacle. As we move toward the west (east) the obstacle becomes taller (shallower) and *Fr* would become smaller (larger). For this value of *Fr*, the fluid parcel ascending the obstacle accelerates as the free surface drops. If there is sufficient increase in velocity and decrease in thickness as the fluid ascends toward the crest, a transition from subcritical to supercritical flow occurs at the top of the obstacle (Blumen, 1990, pp 68). Evidence of this transition is found along the cross section shown in Figure 7and Figure 7c. Thus, the environment is likely to produce wave breaking to the lee side of the Andean bend. It is well known that the wave breaking phenomenon produces significant impacts downslope of the obstacle where it originates (Blumen, 1990). Under these circumstances the flow in the breaking region is turbulent and well-mixed. After the flow passes the crest, the isentropes overturn in a mountain wave and a resonant cavity forms. Downslope flow on the lee side (Figure 7b), is then warmed and mixed and then advected downstream from the bend. The well-mixed air entrains drier air from above the PBL. Subsequently, clear skies form, which in turn allows more radiative warming, and enhancement of the momentum and sensible heat fluxes at the surface.

Different theoretical studies provide clues about the formation of orographically-generated mesoscale vortices in a stable boundary layer (Rotunno et al, 1999; Smolarkiewicz and Rotunno, 1989) and in a well-mixed boundary layer (Crook et al., 1990; Dempsey and Rotunno, 1988; Smith 2003). The main assumptions behind the well-mixed layer theory are wind and potential temperature profiles that remain constant within the layer; conditions that are present in this case (Figure 7a and c). The mixed-layer boundary layer theory also assumes that the flow upstream is uniform so that the horizontal and vertical vorticity is zero. The latter assumption is not true, since the SALLJ has large cyclonic shear close to the Andean foothills (the wind must approach zero as the terrain is approached at any given pressure level.) Thus, there is a sheet of strong cyclonic vorticity close to the foothills, and roughly parallel to it.

The wake produced downstream contains a velocity deficit and associated vertical vorticity. The vorticity equation under the assumption of a well-mixed layer states then that the tilting term cannot generate vertical vorticity since it depends on the presence of horizontal vorticity (or equivalently vertical shear). The dissipation of vorticity by the frictional term also depends on the prior existence of vorticity. Thus, the only term that can generate vertical vorticity without the prior existence of vorticity is the baroclinic term, which involves the gradient of mixing depth and terrain slope (Rotunno et al, 1999). Assuming that the depth of the mixed-layer is constant, we can diagnose the sign and magnitude of the baroclinic vertical vorticity by simply analyzing the cross product between the buoyancy gradient with the gradient of the terrain:

$$Grad(B_{ml}) \times Grad(Z_s),$$

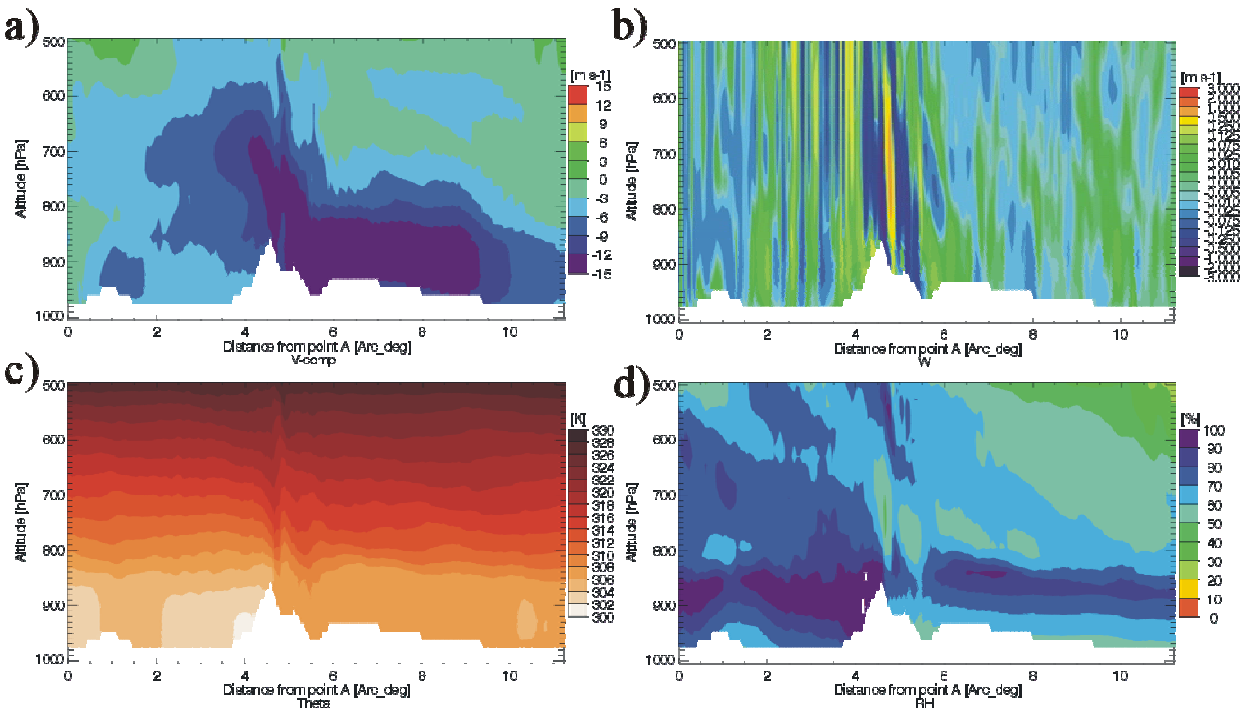

Figure 7 Model-simulated cross-section of meridional wind (a), vertical velocity (b), potential temperature (c), and relative humidity (d) for 1800 UTC. The location of the cross-section (A-B) is indicated in Figure . The white shaded area represents the topography elevation along the trajectory of the flow.

where B_{ml} is the buoyancy field in the mixed-layer and Z_s is the terrain elevation. Figure 8 shows a qualitative analysis where zones of cyclonic vertical vorticity generated by the baroclinic term can occur.

Different problems are identified in the analysis above. First, vertical vorticity due to the horizontal wind gradients (cyclonic vorticity) exit upstream of the Andean bend which is enhanced right at the bend (Figure 5c). Second, the slope of the depth of the mixed-layer is not zero. Although this is not really a problem, it may change the magnitude and perhaps the sign of the vertical vorticity in the analysis. Third, the analysis above also suggests that the intense, concentrated vorticity that develops in the lee of the Andean bend may be also produced by the tilting of horizontal vorticity as gravity waves overturn and break. A more complete vorticity budget will be carried out to evaluate the relative importance of these terms.

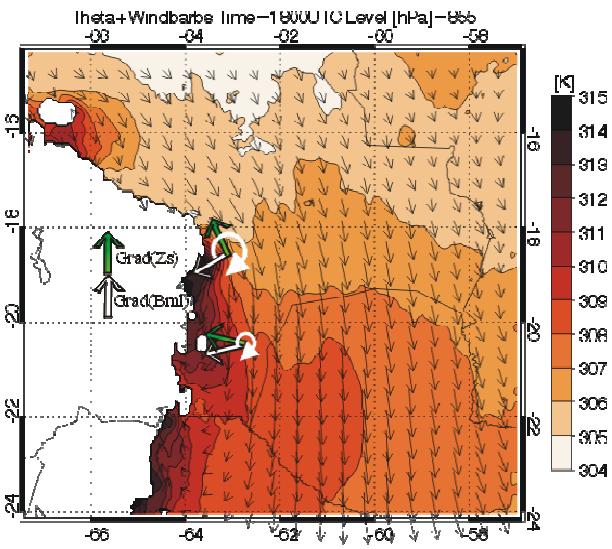

Figure 8 Schematic representation of the baroclinic vertical vorticity generation downstream of the Andean bend. The green thick arrows represent the gradient of sloping terrain and the white one represents the gradient of buoyancy term.

4 SUMMARY AND DISCUSSION

The South American Low-Level Jet (SALLJ) and its interaction with topography has important implications for cloud development along the eastern slopes of the Andes. The dynamics of the flow around the Andean bend during low-level jet events is explored in this study. Generation of vertical vorticity downstream of the Andean bend near Santa Cruz, Bolivia, is significant as it is connected with gravity wave breaking, flow splitting, frictional dissipation and surface drag and it has a long-lived influence on the atmospheric flow patterns downstream of the high terrain.

High-resolution (5 km) simulations show that the flow upstream of the bend is divided at the Andean bend: one part flows around the bend and the other passes over the terrain. The deflected flow can produce regions of convergence and divergence that lead to regions of ascent and subsidence, respectively. The air that flows over the bend produces gravity waves and wave breaking. The wave breaking impacts the airflow downslope of the bend. Turbulent and well-mixed air is expected to form in the breaking region.

A study involving the diurnal variations is necessary to understand better the dynamic of the flow around the Andean bend. A more complete analysis of the P-3 aircraft data during different flights across the Andean bend eddy would also be revealing.

Acknowledgments: NOAA's Office of Global Programs (now Office of Climate Observations) has supported our SALLJEX research. Special thanks to the WRF help support team.

REFERENCES

Barnes, S. L. 1994: Applications of the Barnes Objective Analysis Scheme. Part III: Tuning for Minimum Error. *Journal of Atmospheric and Oceanic Technology*: **Vol. 11**, No. 6, pp. 1459–1479.

Berbery, E., E. Collini, J. Paek,M. Pyle, P. Lonergan, 2002: Mesoscale Diagnosis and Simulation of the South American Monsoon System, EOS. Trans. AGU, 83(47), Fall Meet. Suppl., Abstract A61E-02.

Blumen, W. Ed., 1990: Atmospheric Processes over Complex Terrain. Meteor. Monogr., No. 45, Amer. Meteor. Soc., 323 pp.

Campetella, C. M. and Carolina S. Vera, 2002: The influence of Andes mountains on the South American low-level flow. Geophys. Res. Lett., 29(17), 1826.

Crook, N. Andrew, Clark, Terry L., Moncrieff, Mitchell W. 1990: The Denver Cyclone. Part I: Generation in Low Froude Number Flow. Journal of the Atmospheric Sciences 47: 2725-2742.

Dempsey, David P. and Richard Rotunno. 1988: Topographic Generation of Mesoscale Vortices in Mixed-Layer Models. Journal of the Atmospheric Sciences: 45(20), pp. 2961–2978.

Georgelin, M., and E. Richard, 1996: Numerical simulation of flow diversion around the Pyrenees: a tramontana case study. Mon. Wea. Rev., 124, 687-700.

Stanley L. Barnes. 1994: Applications of the Barnes Objective Analysis Scheme. Part III: Tuning for Minimum Error. Journal of Atmospheric and Oceanic Technology, 11(6), pp. 1459–1479.

Kleeman, R, 1989: A Modeling Study of the Effect of the Andes on the Summertime Circulation of Tropical South America. Journal of the Atmospheric Sciences, 46(21), pp. 3344–3362.

O'Connor, William P. , David H. Bromwich and Jorge F. Carrasco. 1994: Cyclonically Forced Barrier Winds along the Transantarctic Mountains near Ross Island. Mon. Wea. Rev., 122(1), pp. 137–150.

Rotunno, R., Grubiksi´c, V. And Smolarkiewicz, P. K. 1999 Vorticity and potential vorticity in mountain wakes. J. Atmos. Sci., 56, 2796–2810

Smith, R. B, 2003: Advances in mountain airflow dynamics. Preprints, 10th Conf. on Mesoscale Processes, Portland, OR, Amer. Meteor. Soc., 10.1.

Smolarkiewicz, P. K., and R. Rotunno, 1989: Low Froude number flow past three-dimensional obstacles. Part I: Baroclinically generated lee vortices. J. Atmos. Sci., 46, 1154–1164.